

# Computing expectation values of adaptive Fourier density matrices for quantum anomaly detection in NISQ devices

Diego H. Useche, Oscar A. Bustos-Brinez, Joseph A. Gallego,  
Fabio A. González

MindLab Research Group, Universidad Nacional de Colombia, Bogotá, Colombia

E-mail: {diusecher, oabustosb, jagallegom, fagonzalezo}@unal.edu.co

May 2022

## Abstract.

This article presents a novel classical-quantum anomaly detection model based on the expected values of density matrices and a new data embedding called adaptive Fourier features. The method works by estimating a probability density function of training data and classifying new samples as anomalies if they lie below a certain probability density threshold. As a core subroutine, we present a new method to estimate the expected value of a density matrix based on its spectral decomposition on a quantum computer. The anomaly detection model is tested with pure and mixed states and both adaptive and random Fourier features on a synthetic data set for density estimation and on a widely used data set for anomaly detection; results show the superior performance of adaptive Fourier features for density estimation and anomaly detection, and of mixed states for density estimation. An important finding of this work is to show that it is possible to perform anomaly detection with high performance on noise intermediate-scale quantum computers. Code and experiments are available at <https://github.com/diegour1/QuantumAnomalyDetection>.

## 1. Introduction

A problem of interest in many areas of science and engineering is anomaly detection (AD). This problem consists in determining which samples from a given data set are “ordinary” or “normal” (being the interpretation of “normal” defined for each particular case) and which samples depart or are deviated from “normal” data (commonly known as “anomalies”). Some common applications of anomaly detection methods include fraud detection [1] and medical diagnosis [2]. Many classical algorithms have been proposed for AD [3, 4]; however, recent works have shown some advantages of combining quantum computation with AD tasks [5, 6, 7]; for instance, these methods have shown to utilize fewer resources and to present exponential speed-ups in contrast to their classical counterparts.

A well-known approach to performing AD is density estimation (DE), which consists of estimating a probability density function (pdf) of training data to detect anomalous data. Some classical techniques include the ADDE (algorithm detection based on density estimation) [8], and the SmartSifter method, which uses a finite mixture model [9]. Some quantum anomaly detection (QAD) algorithms include the quantum ADDE which operates with amplitude estimation [5, 10], and a quantum clustering method that exploits the variations in the density function to detect anomalies [11].

In this article, we present a novel classical-quantum anomaly detection strategy that combines a density estimation algorithm called density matrix kernel density estimation (DMKDE) [12] with a new quantum representation of data called adaptive Fourier features (AFF). The method induces probability density functions from training data and classifies new samples as “normal” or “anomalies” if they lie either above or below a certain probability threshold.

One of the main results of the article is the statement of a quantum protocol to estimate the expected value of a mixed density matrix in a quantum computer, through a quantum circuit used to implement the prediction phase of the DMKDE. In contrast to methods like quantum state tomography [13, 14, 15] or the variational quantum eigensolver (VQE) [16], which estimate and codify a density matrix in terms of the Pauli matrices, our quantum algorithm uses the spectral decomposition of the density matrix to measure its expected value. In addition, we propose the adaptive Fourier features (AFF), a new trainable quantum feature embedding, based on random Fourier features (RFF) [17], and suitable for both classical and quantum computers. It represents classical data as quantum states, where the inner product in the Hilbert space approximates a Gaussian kernel in the original space. We show that the AFF in conjunction with the DMKDE quantum algorithm allows us to perform density estimation and anomaly detection with a reduced number of components in both a quantum simulator and a real quantum computer. Furthermore, we show that the proposed method is a viable quantum anomaly detection strategy for noise intermediate-scale quantum (NISQ) devices. In sum, the contribution of the article is threefold:

- (i) A new classical-quantum anomaly detection strategy for NISQ computers based on density estimation and the DMKDE algorithm [12].
- (ii) A novel trainable quantum feature mapping called adaptive Fourier features which leverages random Fourier features [18, 17].
- (iii) A new quantum protocol to estimate the expected value of a density matrix based on its diagonal representation.

The outline of the document is as follows: in Sect. 2, we describe the related work; in Sect. 3, we present the theoretical background of the DMKDE algorithm, the RFF, the notation of the quantum circuits, and a previously proposed quantum protocol [19] to estimate the expected value of a density matrix of a pure state; in Sect. 4, we introduce our proposed quantum anomaly detection method, outline the proposed quantum circuit to estimate the expected value of a mixed state density matrix, and

show the proposed adaptive Fourier features; in Sect. 5, we illustrate the results of our proposed method for density estimation and anomaly detection; and in Sect. 6, we establish our conclusions and future outlook.

## 2. Related Work

Anomaly detection is an important problem in machine learning and solving it using quantum computers is an interesting challenge for the field of quantum machine learning. Recent approaches to quantum anomaly detection (QAD) include variational quantum algorithms, for instance, Herr et al. [7] use the variational method in conjunction with quantum generative adversarial networks, and in Ref. [20], they combine the variational quantum eigensolver with quantum autoencoders. In the non-variational side, some proposals perform QAD with quantum clustering [21, 11], and build density functions from data with multivariate Gaussian distributions [5, 10].

Besides VQE-based algorithms, most quantum machine learning methods are based on pure states. One QAD method based on mixed states was proposed by Liu et. al. [6], they proposed a quantum one-class support vector machine, which codifies the density matrix based on the Krauss operators. Our proposed method is also based on mixed states, by estimating the expected values of density matrices.

If we consider a density matrix as an operator, its expectation value is equivalent to a quantum state overlap between a pure state and the mixed state density matrix. The most commonly used protocol for quantum state projection is the swap test [22] which was conceived to find the state overlap between pure states, in Ref. [23], they showed that this protocol can also be used for mixed states. Other protocols to measure the state overlap were proposed in Refs. [19, 24]. In addition, the VQE method [16] can estimate the expected value of a density matrix, by writing the quantum state in terms of the Pauli matrices. Our method departs from the aforementioned techniques, by estimating the expected value of a density matrix from its spectral decomposition.

González et. al. [18] proposed the use of random Fourier features (RFF) [17] as quantum feature maps. RFF approximates shift-invariant kernels by calculating an explicit mapping to a low-dimensional feature space. Enhancing the capability of random Fourier features to approximate shift-invariant kernels is an active area of research. Two of the main approaches to the problem include refining the original RFF Montecarlo sampling and using optimization techniques to find the optimal Fourier parameters. Regarding the RFF sampling, Kammonen et. al. [25] proposed a method to find non-Gaussian Fourier features based on Metropolis-hastings, also Ref. [26] proposed reducing the number of features by the kernel polarization method [27]. Other methods include a surrogate leverage sampling based on kernel alignment [28], compressing the dimension of the RFF by using only a subset of features which reduces the Fobrenius norm error [29], and using a multilayer generative network to select the optimal sampled Fourier weights [30].

On the optimization side, there have been multiple proposals that use neural

networks to make the parameters of the random Fourier features trainable. For instance, Li et. al. [31] proposed learnable Fourier features in conjunction with dense networks for positional encoding, and Ref. [32] propose the RFFNET, a deep learning architecture that trains layers of RFF for kernel learning. Other methods for kernel learning include using LSTM to learn the parameters of the RFF [33], learning the RFF weights for multiple kernel learning [34] and employing a generative adversarial network to translate the RFF sampling from a base Gaussian distribution to more complex distributions [35]. In addition, Ref. [36] proposed a method to find the peaks in the Fourier parameters which maximize kernel alignment. Our adaptive Fourier features technique can be framed in this last category of methods, but using a siamese network to find the optimal parameters which reduce the mean squared distance between the expected kernel and its Fourier feature approximation. These optimized features are then used to construct pure and mixed quantum states for quantum anomaly detection.

### 3. Preliminaries

In this section, we present the DMKDE algorithm proposed by Gonzalez et al. [12], which is a non-parametric density estimation method based on density matrices and random Fourier features [17], and a special case of the quantum measurement classification algorithm (QMC) [18]. In particular, we describe two approaches to the method: pure and mixed states. Additionally, we explain the notation of the quantum circuits used through the article and present a previous work [19] to compute the expected value of a pure state density matrix in a quantum computer.

#### 3.1. Density Matrix Kernel Density Estimation and Random Fourier Features

The machine learning algorithm density matrix kernel density estimation (DMKDE) [12] constructs a density matrix from training data and estimates the probability density of a test sample by computing the expected value of the test state with the training density matrix.

The method starts by applying a quantum feature map, based on random Fourier features [17, 18], to each sample in the train and test data set  $\mathbf{x}_i \rightarrow |\psi_i\rangle$ , where  $\mathbf{x}_i \in \mathbb{R}^D$  and  $|\psi_i\rangle \in \mathbb{R}^d$  with  $\langle \psi_i | \psi_i \rangle = 1$ . The RFF technique creates a quantum embedding whose inner product approximates a shift-invariant positive definite kernel; in this article we use the Gaussian kernel  $k(\mathbf{x} - \mathbf{y}) = e^{-\gamma|\mathbf{x} - \mathbf{y}|^2}$ . The parameters of the RFF are the inverse of the variance of the Gaussian kernel, denoted by  $\gamma$  (gamma), and the dimension of the quantum features  $d$ .

Once the random Fourier feature map is established, the DMKDE method explores two approaches to train the density matrix; pure and mixed states. For the training states  $|\psi_i\rangle$  for  $i \in \{1, \dots, N\}$ , the pure state training density matrix is computed by,

$$|\phi_{\text{train},1}\rangle = \frac{\sum_i |\psi_i\rangle}{|\sum_i |\psi_i\rangle|}, \quad \text{and} \quad \rho_{\text{train},1} = |\phi_{\text{train},1}\rangle \langle \phi_{\text{train},1}|, \quad (1)$$

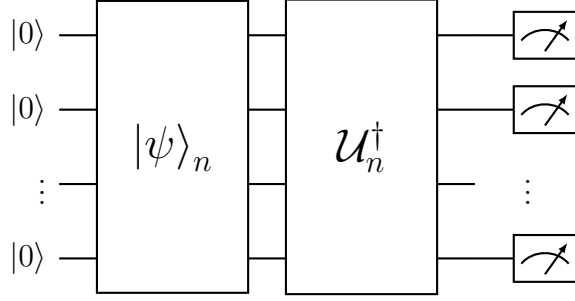


Figure 1: DMKDE quantum circuit for pure states [19].

and, the mixed state by,

$$\rho_{\text{train},2} = \frac{1}{N} \sum_{i=1}^N |\psi_i\rangle \langle \psi_i|, \quad (2)$$

the indices 1 and 2 refer to pure and mixed approaches respectively. The probability density estimators of a testing sample  $\mathbf{x} \rightarrow |\psi\rangle$  are computed by,

$$\hat{p}_1(|\psi\rangle) = C_{\gamma,1} \sqrt{\langle \psi | \rho_{\text{train},1} | \psi \rangle} = C_{\gamma,1} \sqrt{|\langle \phi_{\text{train},1} | \psi \rangle|^2}, \quad (3)$$

$$\hat{p}_2(|\psi\rangle) = C_{\gamma,2} \langle \psi | \rho_{\text{train},2} | \psi \rangle, \quad (4)$$

where  $C_{\gamma,1}$  and  $C_{\gamma,2}$  are normalization constants that depend on the parameter  $\gamma$ .

The DMKDE algorithm in conjunction with RFF is an efficient approximation of the Parzen–Rosenblatt window [37, 38], a non-parametric method for density estimation. In this document, we consider the DMKDE with RFF [12] as a baseline for the proposed classical-quantum implementation of the DMKDE with adaptive Fourier features (discussed in Sect. 4.1).

### 3.2. Notation and DMKDE quantum circuit for pure states

We now introduce the notation of the quantum circuits used in the article, which is the same notation used in Ref. [39]. Any state of the canonical basis of an  $n$ -qubit state can be written as  $|b_0 b_1 \cdots b_{n-1}\rangle$  with  $b_i \in \{0, 1\}$ , hence, we may write any state in the canonical basis as a string in its binary form. This notation can be simplified by writing such state as  $|\sum_{i=0}^{n-1} b_i 2^i\rangle_n$ , namely, the bit-string is written in decimal form and the subindex indicates the number of qubits of the state. For example, the 4-qubit state  $|1010\rangle$  can be written as  $|5\rangle_4$ . We make use of the same subindex to illustrate the number of qubits upon which a unitary gate or a quantum state initialization acts.

Once established the notation of the circuits, we present a previously proposed quantum circuit by Liu et al. [19] to compute the expected value of a pure state density matrix, which is equivalent to calculating the inner product of two pure quantum states,

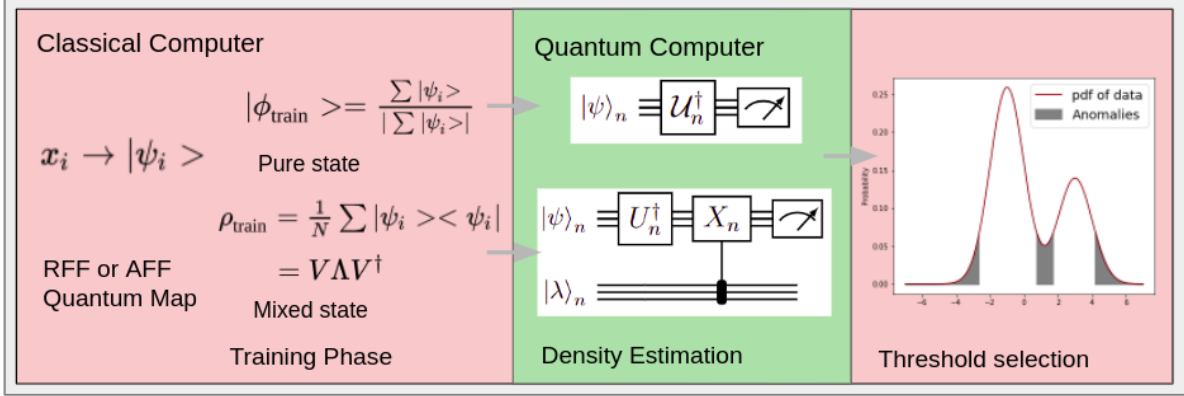


Figure 2: Classical-quantum anomaly detection model.

as indicated by Eq. 3. The circuit starts by initializing a  $n$ -qubit state with the state  $|\psi\rangle_n \in \mathbb{C}^d$ , with  $2^{n-1} < d \leq 2^n$ , by means of amplitude encoding [40], and then it applies a unitary matrix  $\mathcal{U}_n^\dagger$ , which satisfies that  $\mathcal{U}_n |0\rangle_n = |\phi_{\text{train},1}\rangle_n$ , see Eq. 1 and Figure 1. By measuring all the  $n$  qubits, the probability of the state  $|0\rangle_n$  is the expected value of a pure state density matrix, i.e.  $P(|0\rangle_n) = |\langle \phi_{\text{train},1} | \psi \rangle|^2$ . Other quantum techniques to measure the fidelity of quantum states can be seen in Refs. [22, 24]. In this article, we present a new quantum protocol to estimate the expected value of a mixed state density matrix based on its eigendecomposition in a qubit-based quantum computer.

#### 4. Quantum anomaly detection method

We propose a hybrid classical-quantum model for anomaly detection based on the DMKDE algorithm [12] and the novel adaptive Fourier features technique. Fig. 2 shows the main steps of the method: (i) quantum feature map, (ii) training phase, (iii) density estimation of new samples, and (iv) threshold selection and classification. The steps (i), (ii), and (iv) are calculated in a classical computer, while the step (iii) is computed in a real quantum computer and a quantum simulator. These steps are explained in more detail below.

- (i) Quantum feature map: Given a dataset to classify, split it into three partitions: train, validation, and test, in such a way that each of them is composed of both “normal” and “outlier” data. Then apply a quantum feature map  $x_i \rightarrow |\psi_i\rangle$  to all of these partitions; the selected embedding from data to quantum states can be based on the proposed adaptive Fourier features, see Sect 4.1, or on random Fourier features [17, 18].
- (ii) Training phase: Use the training data to compute either the training quantum state  $|\phi_{\text{train},1}\rangle$  for the pure state or the training density matrix  $\rho_{\text{train},2}$  for the mixed state, see Equations 1 and 2. When using the mixed state approach, also calculate the spectral decomposition of the training density matrix  $\rho_{\text{train},2} = V\Lambda V^\dagger$ . The

training pure and mixed quantum states encode probability distributions of the training dataset.

- (iii) Density estimation of new samples: Estimate the probability density values of the validation and test partitions by computing the probability estimation of the samples with the training density matrix. The estimator of the pure state (see Eq. 3) is obtained using the quantum circuit shown in Fig. 1 [19]. To calculate the probability estimator of a mixed state (see Equation 4), use the proposed quantum circuit shown in Fig. 3. See Sect. 4.2 for the mathematical details of the mixed state quantum circuit.
- (iv) Threshold selection: Once given the probability density estimations, use the validation dataset to select a threshold to separate the samples: if a sample has a density lower than the threshold, then it is considered an “outlier”. Since the validation samples include both normal data and outliers, the threshold must be somewhere between the maximum and minimum density values; the specific threshold value to choose is found using percentiles, but other metrics can be used. Finally, use this threshold to classify the samples in the test partition.

In the next sections, we present the theoretical details of the new adaptive Fourier features method, and the proposed DMKDE quantum protocol to compute the expected value of a mixed state density matrix.

#### 4.1. Adaptive Fourier Features Quantum Feature map

To build the quantum features of the classical-quantum anomaly detection strategy, we propose the adaptive Fourier features (AFF) technique: a new trainable feature embedding based on random Fourier features [17], which maps classical data samples  $\mathbf{x} \in \mathbb{R}^D$  to quantum state-like representations  $|\psi\rangle \in \mathbb{R}^d$ , where the inner product on the quantum feature space approximates a positive definite shift-invariant kernel on the original space. In this work, we use the Gaussian kernel given by  $k(\mathbf{x}, \mathbf{y}) = e^{\gamma|\mathbf{x}-\mathbf{y}|^2}$ .

In general terms, the method utilizes the training data set  $\mathcal{X}$  in the original space to train the parameters of the adaptive Fourier features, hence obtaining a quantum state-like representation of the data. The AFF method involves the following steps: (i) build a synthetic data set, composed of two random orderings of the original data set, where the labels are formed by computing the Gaussian kernel between these two subsets, (ii) construct a siamese neural network and initialize its parameters using conventional random Fourier features, (iii) train the siamese network with the synthetic data set to adjust the parameters of the adaptive Fourier features, (iv) make predictions on the original data set to obtain the AFF representations.

As mentioned before the strategy for AFF starts by creating two random shuffles  $\mathcal{X}_1$  and  $\mathcal{X}_2$  of the original data set  $\mathcal{X}$ , with  $N$  training samples, and then computing the Gaussian kernel between these two subsets to form the synthetic set of labels  $y_i \in \mathcal{Y}$ ,

for  $i \in \{1, \dots, N\}$ , such that,

$$y_i = \exp(\gamma_s |\mathbf{x}_{i,1} - \mathbf{x}_{i,2}|^2), \quad (5)$$

with  $\gamma_s$  the shape parameter of the kernel, and  $\mathbf{x}_{i,1}$  and  $\mathbf{x}_{i,2}$  the  $i^{\text{th}}$  sample vectors of  $\mathcal{X}_1$  and  $\mathcal{X}_2$  respectively.

Next, we build a siamese neural network with a trainable weight matrix  $W \in \mathbb{R}^{d \times D}$ , whose weights are initialized by sampling a normal distribution  $\mathcal{N}(0, 1)$ , and then multiplying the weight matrix by a factor of  $\sqrt{2\gamma}$ , this factor establish the Gaussian spread of the Fourier features, the inverse of the variance of the Fourier features  $\gamma$  might differ from the shape parameter  $\gamma_s$ , also a trainable bias vector  $\mathbf{b} \in \mathbb{R}^d$  is initialized by sampling from a uniform distribution  $\mathcal{U}(0, 2\pi)$ . The forward pass to obtain the adaptive Fourier features resembles conventional RFF:

$$\mathbf{z}(\mathbf{x}) = \sqrt{2/d} \cos \left[ \left( \sqrt{2\gamma} W \right) \mathbf{x} + \mathbf{b} \right], \quad |\psi\rangle = \frac{\mathbf{z}(\mathbf{x})}{|\mathbf{z}(\mathbf{x})|}. \quad (6)$$

We then use the synthetic data set composed of  $\mathcal{X}_1$ ,  $\mathcal{X}_2$  and  $\mathcal{Y}$  to train the siamese network. We use the *Mean Squared Error* (MSE) loss function to find the optimal parameters  $W$  and  $\mathbf{b}$  of the network,

$$\mathcal{L} = \frac{1}{N} \sum_{i=1}^N (y_i - |\langle \psi_{i,1} | \psi_{i,2} \rangle|^2)^2. \quad (7)$$

Finally, the quantum state-like representation with adaptive Fourier features is obtained by making predictions on the original data set  $\mathcal{X}$ , see Eq. 6.

#### 4.2. DMKDE quantum circuit for mixed states

To implement the prediction phase of the DMKDE, see Eq. 4, we also propose a novel quantum protocol to estimate the expected value of a mixed state density matrix in a qubit-based quantum computer. This circuit extends to qubits a previous implementation of the mixed state DMKDE in a high-dimensional quantum computer [41], and to mixed states, a previous implementation of the DMKDE with pure states in a qubit-based quantum computer [42, 19].

We want to compute the expected value of a density matrix  $\rho \in \mathbb{C}^{d \times d}$  with a quantum state  $|\psi\rangle \in \mathbb{C}^d$  in a quantum computer. This calculation requires  $2 \times n$  qubits, with  $2^{n-1} < d \leq 2^n$ . The first  $n$  qubits encode the state  $|\psi\rangle$  and the unitary matrix  $V^\dagger$  whose rows are the complex conjugate eigenvectors of  $\rho$ , and the remaining  $n$  qubits encode the eigenvalues of the density matrix.

To begin with, as noted in [41], we have that,

$$\langle \psi | \rho | \psi \rangle = \langle \psi | V \left( \sum_{i=0}^{d-1} \lambda_i |i\rangle \langle i| \right) V^\dagger | \psi \rangle = \sum_{i=0}^{d-1} \lambda_i |\langle i | V^\dagger | \psi \rangle|^2, \quad (8)$$

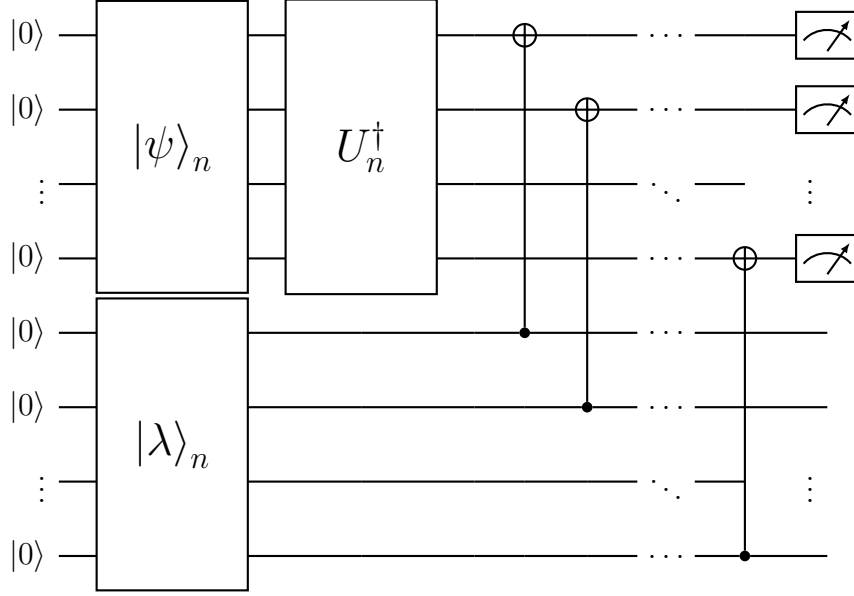


Figure 3: DMKDE quantum circuit for mixed states.

where,  $V \in \mathbb{C}^{d \times d}$  is the unitary matrix of eigenvectors and  $\Lambda = \sum_{i=0}^{d-1} \lambda_i |i\rangle \langle i|$  is the diagonal matrix of eigenvalues.

The proposed DMKDE quantum circuit starts by initializing the first  $n$  qubits with the state  $|\psi\rangle_n$ , see the notation in Sect. 3.2, and the remaining  $n$  qubits with the state  $|\lambda\rangle_n = \sum_{i=0}^{d-1} \sqrt{\lambda_i} |i\rangle_n$ , state that encodes the eigenvalues of  $\rho$ , see Fig. 3. This operation can be performed thanks to amplitude encoding [40]. We have that,

$$|\psi\rangle_n \otimes |\lambda\rangle_n = |\psi\rangle_n \otimes \sum_{i=0}^{d-1} \sqrt{\lambda_i} |i\rangle_n. \quad (9)$$

Next, we construct a unitary matrix  $U_n^\dagger$ , see Eq. 10, whose first quadrant is composed of the unitary matrix  $V^\dagger$  and its fourth quadrant with the identity matrix  $I_{2^{n-d}}$ ,

$$U_n^\dagger = \left( \begin{array}{c|c} V^\dagger & \\ \hline & I_{2^{n-d}} \end{array} \right), \quad (10)$$

this unitary matrix  $U_n^\dagger$  is applied to the first  $n$  qubits in the form of an isometry [39]. We would have,

$$U_n^\dagger |\psi\rangle_n \otimes \sum_{i=0}^{d-1} \sqrt{\lambda_i} |i\rangle_n. \quad (11)$$

We can write the state of the first  $n$  qubits as,  $U_n^\dagger |\psi\rangle_n = \sum_{i=0}^{d-1} a_i |i\rangle_n$ . Where,

$$|a_i|^2 = |\langle i|_n U_n^\dagger |\psi\rangle_n|^2 = |\langle i| V^\dagger |\psi\rangle|^2, \quad (12)$$

namely,  $|a_i|^2$  is the probability to measure  $U_n^\dagger |\psi\rangle_n$  in the canonical state  $|i\rangle_n$ . Therefore, the circuit leads,

$$\begin{aligned} U_n^\dagger |\psi\rangle_n \otimes |\lambda\rangle_n &= \sum_{i=0}^{d-1} a_i |i\rangle_n \otimes \sum_{j=0}^{d-1} \sqrt{\lambda_j} |j\rangle_n \\ &= \sum_{i=0}^{d-1} a_i \sqrt{\lambda_i} |i\rangle_n \otimes |i\rangle_n + \sum_{\{(i,j):i \neq j\}} a_i \sqrt{\lambda_j} |i\rangle_n \otimes |j\rangle_n. \end{aligned}$$

We then apply a cascade of  $n$  CNOT gates, between the first and the second halves of the circuit, as shown in Fig. 3. The  $i^{\text{th}}$  CNOT operates with control the  $(i+n)^{\text{th}}$  qubit and target the  $i^{\text{th}}$  qubit, with  $i \in \{0, \dots, n-1\}$ . The effect of this series of CNOT gates can be observed by writing,

$$|i\rangle_n \otimes |j\rangle_n = \left| \sum_{k=0}^{n-1} b_k^i 2^k \right\rangle_n \otimes \left| \sum_{l=0}^{n-1} b_l^j 2^l \right\rangle_n, \quad (13)$$

where,  $|b_0^i b_1^i \dots b_{n-1}^i\rangle$  and  $|b_0^j b_1^j \dots b_{n-1}^j\rangle$  are the binary representations of  $|i\rangle_n$  and  $|j\rangle_n$  respectively. The  $n$  CNOT gates have the same complexity as a single CNOT, as they can be parallelized in a quantum computer [24].

We represent this series of  $n$  CNOT gates with the  $2n$ -qubit unitary operation  $U_{2n}^{\text{Cnot}}$ . The outcome of this transformation is a qubit-wise summation modulo 2 (denoted by  $\oplus$ ) on the first half of the circuit,

$$U_{2n}^{\text{Cnot}}(|i\rangle_n \otimes |j\rangle_n) = \left| \sum_{k=0}^{n-1} (b_k^i \oplus b_k^j) 2^k \right\rangle_n \otimes \left| \sum_{l=0}^{n-1} b_l^j 2^l \right\rangle_n. \quad (14)$$

If  $i = j$ , we would have that,

$$U_{2n}^{\text{Cnot}}(|i\rangle_n \otimes |i\rangle_n) = |0\rangle_n \otimes \left| \sum_{l=0}^{n-1} b_l^i 2^l \right\rangle_n \quad (15)$$

In contrast, if  $i \neq j$ , the state  $\left| \sum_k (b_k^i \oplus b_k^j) 2^k \right\rangle_n$  would be distinct to the  $|0\rangle_n$  state.

Therefore, after applying the series of  $n$  CNOT gates, the resulting state of the DMKDE quantum circuit is,

$$\sum_{i=0}^{d-1} a_i \sqrt{\lambda_i} |0\rangle_n \otimes |i\rangle_n + \sum_{\{(i,j):i \neq j\}} a_i \sqrt{\lambda_j} \left| \sum_k (b_k^i \oplus b_k^j) 2^k \right\rangle_n \otimes |j\rangle_n. \quad (16)$$

By measuring the first  $n$  qubits the probability of state  $|0\rangle_n$  would be,

$$P(|0\rangle_n) = \sum_{i=0}^{d-1} |a_i|^2 \lambda_i = \sum_{i=0}^{d-1} \lambda_i |\langle i | V^\dagger |\psi\rangle|^2 = \langle \psi | \rho | \psi \rangle, \quad (17)$$

see Eqs. 8 and 12.

## 5. Results

### 5.1. Quantum density estimation

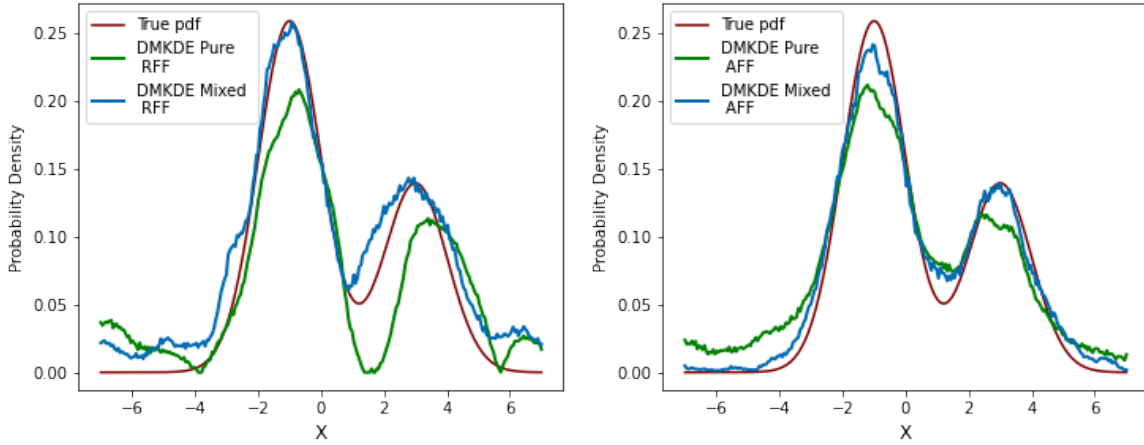
As mentioned in Sect. 3, the DMKDE algorithm along with the RFF embedding [12] encodes in a density matrix a probability distribution of the training data and estimates the probability density of new testing samples. Therefore, the algorithm can be used to approximate probability density functions.

To test the DMKDE algorithm with the new adaptive Fourier features and the proposed DMKDE quantum circuit for mixed states, we constructed a one-dimensional probability density function corresponding to a mixture of two Gaussians. The training data set was composed of 1000 points sampled from the pdf, and the testing data set was formed by 250 equidistant points. Two quantum feature maps based on AFF and RFF were applied to both train and test data sets, we chose features of 16 components with  $\gamma = 1$ , for both adaptive and random features. We found that a value of  $\gamma$  with the same order of magnitude as the inverse of the variance of the training data was appropriate for density estimation. For each quantum feature embedding, we constructed pure and mixed training density matrices of dimensions 16x16, see Eqs. 1 and 2. For the prediction step, we computed the probability density estimator for both pure and mixed states, see Eqs. 3 and 4; the pure state estimator was computed with the circuit proposed by Liu et al. [19], see Fig. 1, and the mixed state estimator with our proposed DMKDE quantum circuit, see Fig. 3. In total, we report 4 experiments, one for each configuration, with the Qiskit QASM simulator of the IBM-Qiskit platform.

In Fig. 4, we show the probability density estimation for pure and mixed states with both random and adaptive Fourier features. In comparison with the pure state, the mixed state creates a better approximation of the pdf for both quantum embeddings, especially, in high-density regions. We found also better and less noisy results with AFF compared with RFF. It should be highlighted that for RFF, we chose the best performing features for density estimation, out of 20 random Fourier configurations; in contrast, for AFF, we obtained satisfactory density estimation results through multiple training iterations. To improve the estimation of the pdf and reduce the noise in low-density regions, it is required a higher number of Fourier features and henceforth bigger density matrices.

### 5.2. Quantum anomaly detection

Once the ability of the proposed circuits to approximate probability density functions was established, a similar experiment was performed with a previously labeled anomaly detection dataset. For this purpose, we used a modified version, from Ref. [43], of the Cardiotocography dataset from the UCI Machine Learning Repository, related to fetal heart rate. It consists of 1831 samples, where each sample contains 21 attributes, with two classes: the *normal* class for the inliers, and the *pathologic* class for the outliers. This dataset was divided into three partitions: train (60%), validation (20%), and test



(a) Density estimation with random Fourier features.

(b) Density estimation with adaptive Fourier features.

Figure 4: Density estimation with both pure and mixed states and random and adaptive Fourier features. The DMKDE experiments for density estimation were performed with the Qiskit QASM simulator applied to a 4-qubit DMKDE circuit for pure states, and a 8-qubit DMKDE circuit for mixed states. Both approaches have 16 Fourier features.

(20%), all of which contained both normal samples and outliers in the same proportion (approximately, 9.6% of all samples were labeled as outliers).

As a first step, RFF and AFF were applied to the samples of all partitions as quantum feature mappings. To evaluate the effect of the number of Fourier features on the classification, we worked with 4 and 8 dimensions (which, once normalized, corresponded to quantum states of 2 and 3 qubits, respectively). With the quantum states of the training partition samples, we calculated the density matrices for pure states  $\rho_{train,1}$  (see Eq. 1) and for mixed states  $\rho_{train,2}$  (see Eq. 2), and then we used them to build the respective quantum circuits. As usual in anomaly detection algorithms, labels were not used during the training phase.

These circuits were then run on the Qiskit QASM simulator, performing an iteration of the circuit for each sample in validation and test partitions to obtain the density estimates for all samples. After obtaining the density values, the classification of each one as “normal” or “outlier” required comparing its density value with a threshold value  $t$ . The search for the threshold was performed over the validation partition, by setting a percentile value  $t$  such that 9.6% of the samples lay below it, thus being considered anomalies. We then used the obtained boundary  $t$  to classify the testing samples.

In Ref. [12], the authors highlight the influence of the  $\gamma$  parameter used in RFF mapping for the performance of a classifier. For this reason, we searched for the optimal values of  $\gamma_s$  and  $\gamma$  in a logarithmic scale (considering only powers of two ranging from  $2^{-10}$  to  $2^0$ ); hence, in all scenarios, we set  $\gamma_s = 2^{-6}$  and  $\gamma = 2^{-7}$  as the best values for AFF, and  $\gamma = 2^{-7}$  for RFF. For each RFF and AFF quantum embedding, we used the

same features for the pure and mixed state approaches. We simulated each circuit ten times, randomizing the RFF embedding and the initial parameters of the AFF mapping.

Then, we report the average accuracy, AUC (area under the characteristic curve), and F1 Score of the “anomalous” class, for ten experiments for each classifier, both for 4 and 8 dimensions with RFF and AFF, with both pure and mixed state approaches. The metrics were calculated using functions provided in the scikit-learn Python library. The results are presented in Table 1. We found no significant difference in performance between pure and mixed state approaches. Differences are more noticeable when considering the dimensionality of the mapping and the type of encoding: RFF of size 8 obtained better results compared to RFF of size 4, also AFF with 4 components had a slightly better performance compared to AFF with 8 components. This indicates that an increase in the RFF components improves the performance of the algorithm, in contrast, AFF can achieve satisfactory results with a low number of features. Regarding the standard deviations, we observe more consistent results across different experiments with AFF. Therefore, it shows that RFF is more sensible to randomness than AFF in a low-dimensional setting. The random initialization of the AFF was attenuated thanks to the neural network learning.

Size	Method	F1 Score	Accuracy	AUC
RFF: 4	Pure	$0.3751 \pm 0.1415$	$0.8823 \pm 0.0208$	$0.7661 \pm 0.1133$
	Mixed	$0.3802 \pm 0.1483$	$0.8839 \pm 0.0215$	$0.7696 \pm 0.1144$
AFF: 4	Pure	$0.6843 \pm 0.0311$	$0.9409 \pm 0.0044$	<b><math>0.9634 \pm 0.0049</math></b>
	Mixed	<b><math>0.6967 \pm 0.0212</math></b>	<b><math>0.9414 \pm 0.0041</math></b>	$0.9624 \pm 0.0036$
RFF: 8	Pure	$0.4814 \pm 0.1003$	$0.9033 \pm 0.0158$	$0.8702 \pm 0.0722$
	Mixed	$0.4772 \pm 0.1007$	$0.9035 \pm 0.0159$	$0.8731 \pm 0.0703$
AFF: 8	Pure	$0.6607 \pm 0.0269$	$0.9343 \pm 0.0048$	$0.9593 \pm 0.0028$
	Mixed	$0.6487 \pm 0.0384$	$0.9316 \pm 0.0077$	$0.9592 \pm 0.0030$

Table 1: Obtained metrics for quantum anomaly detection experiments using RFF and AFF with QASM Simulator.

We also performed some of these experiments on real noisy quantum hardware, accessible through the IBM-Quantum platform; we aimed to determine that our algorithm is a feasible approach for near-term quantum computers [44], by studying its sensitivity to quantum noise. Given the satisfactory performance and the available quantum hardware, we restricted the experiments to RFF and AFF with four components, these quantum circuits required two qubits for the pure state scenario and four qubits for the mixed state scenario.

As before, we report the accuracy, AUC, and F1 Score of the anomalous class for each case; since our experiments required a different circuit for each sample in validation and test partitions, we performed these experiments once, thus obtaining a unique value for each metric. Results are presented in Table 2. The results follow a similar

pattern as the quantum simulator: AFF leads to higher performance in comparison to RFF. However, when comparing pure and mixed state approaches, there is a noticeable advantage of the pure state; this can be explained in terms of the complexity of the quantum circuits, for instance, the pure state approach requires half of the number of qubits of the mixed state approach, hence, it might have a lower sensitivity to noise.

Size	Method	F1 Score	Accuracy	AUC
RFF: 4	Pure	0.4286	0.8910	0.7945
	Mixed	0.3768	0.8828	0.7856
AFF: 4	Pure	<b>0.7246</b>	<b>0.9482</b>	<b>0.9681</b>
	Mixed	0.6111	0.9237	0.9418

Table 2: Obtained metrics for the quantum anomaly detection experiments using IBM quantum computers (IBMQ-Quito and IBMQ-Santiago) with RFF and AFF for both pure and mixed states.

## 6. Conclusions

In this article, we presented a classical-quantum anomaly detection model, based on the density matrix kernel density estimation algorithm proposed by Gonzalez et al. [12], and the new data embedding called adaptive Fourier features. Our proposed AD technique works by estimating a probability density function from training data and classifying test data as “normal” or “outlier” by setting a probability threshold in the pdf that acts as a boundary between these regions. Within our AD method, we proposed the DMKDE quantum protocol, which estimates the expected value of any eigen-decomposed density matrix in a quantum computer with a logarithmic number of resources; and the adaptive Fourier features a new trainable representation of data, based on RFF [18, 17], which allows for a low-dimensional representation of data.

We explored four approaches within our method to perform the estimations: pure and mixed states with both random and adaptive Fourier features. We then applied them for two different purposes, density estimation of a given pdf function and anomaly detection on a dataset; we evaluated the model with quantum features of 4 and 8 dimensions for anomaly detection, and with 16 dimensions for density estimation. In comparison to conventional RFF, AFF demonstrated superior performance on both density estimation and anomaly detection, being able to estimate probability density functions with a low number of components. In addition, the results indicated a small advantage of the mixed state approach for density estimation. However, the use of pure or mixed states for quantum anomaly detection is not conclusive: the mixed state approach might be preferred on noise-free devices, while the pure state approach would be favored on real quantum computers. The experimental results show that the proposed QAD method is a feasible approach for noise intermediate-scale quantum computers.

Future work of the proposed classical-quantum AD technique includes comparing the performance of our method with other classical and quantum anomaly detection methods, and also increasing the number of Fourier features, hence augmenting the size of the quantum circuits (given the near-term limitations in quantum hardware). Besides, we aim to apply adaptive Fourier features as mapping functions to other kernel methods and to study its theoretical implications and performance. An interesting future endeavor involves integrating the proposed DMKDE quantum circuit with variational quantum algorithms to learn mixed quantum states in a quantum computer.

## Acknowledgments

We acknowledge the use of IBM Quantum services for this work. The views expressed in this work are those of the authors and do not reflect the official policy or position of IBM or the IBM Quantum team.

## References

- [1] Véronique Van Vlasselaer, Cristián Bravo, Olivier Caelen, Tina Eliassi-Rad, Leman Akoglu, Monique Snoeck, and Bart Baesens. APATE: A novel approach for automated credit card transaction fraud detection using network-based extensions. *Decision Support Systems*, 75:38–48, 7 2015. ISSN 0167-9236. doi: 10.1016/J.DSS.2015.04.013.
- [2] Li Fei Chen. An improved negative selection approach for anomaly detection: with applications in medical diagnosis and quality inspection. *Neural Computing and Applications 2011 22:5*, 22(5):901–910, 12 2011. ISSN 1433-3058. doi: 10.1007/S00521-011-0781-5. URL <https://link.springer.com/article/10.1007/s00521-011-0781-5>.
- [3] Caleb C. Noble and Diane J. Cook. Graph-based anomaly detection. *Proceedings of the ACM SIGKDD International Conference on Knowledge Discovery and Data Mining*, pages 631–636, 2003. doi: 10.1145/956750.956831.
- [4] Fabio A. González and Dipankar Dasgupta. Anomaly Detection Using Real-Valued Negative Selection. *Genetic Programming and Evolvable Machines 2003 4:4*, 4(4):383–403, 12 2003. ISSN 1573-7632. doi: 10.1023/A:1026195112518. URL <https://link.springer.com/article/10.1023/A:1026195112518>.
- [5] Jin Min Liang, Shu Qian Shen, Ming Li, and Lei Li. Quantum anomaly detection with density estimation and multivariate Gaussian distribution. *Physical Review A*, 99(5):052310, 5 2019. ISSN 24699934. doi: 10.1103/PHYSREVA.99.052310/FIGURES/1/MEDIUM. URL <https://journals.aps.org/pr/abstract/10.1103/PhysRevA.99.052310>.
- [6] Nana Liu and Patrick Rebentrost. Quantum machine learning for quantum anomaly detection. *Physical Review A*, 97(4):042315, 4 2018. ISSN 24699934.

- doi: 10.1103/PHYSREVA.97.042315/FIGURES/1/MEDIUM. URL <https://journals.aps.org/prab/abstract/10.1103/PhysRevA.97.042315>.
- [7] Daniel Herr, Benjamin Obert, and Matthias Rosenkranz. Anomaly detection with variational quantum generative adversarial networks. *Quantum Science and Technology*, 6(4):045004, 7 2021. ISSN 2058-9565. doi: 10.1088/2058-9565/AC0D4D. URL <https://iopscience.iop.org/article/10.1088/2058-9565/ac0d4dhttps://iopscience.iop.org/article/10.1088/2058-9565/ac0d4d/meta>.
- [8] Markus M. Breunig, Hans-Peter Kriegel, Raymond T. Ng, and Jörg Sander. LOF: Identifying Density-Based Local Outliers. *Proceedings of the 2000 ACM SIGMOD international conference on Management of data - SIGMOD '00*, pages 93–104, 2000. doi: 10.1145/342009.335388. URL <http://portal.acm.org/citation.cfm?doid=342009.335388>.
- [9] Kenji Yamanishi, Jun Ichi Takeuchi, Graham Williams, and Peter Milne. On-Line Unsupervised Outlier Detection Using Finite Mixtures with Discounting Learning Algorithms. *Data Mining and Knowledge Discovery 2004 8:3*, 8(3):275–300, 5 2004. ISSN 1573-756X. doi: 10.1023/B:DAMI.0000023676.72185.7C. URL <https://link.springer.com/article/10.1023/B:DAMI.0000023676.72185.7c>.
- [10] Ming-Chao Guo, Hai-Ling Liu, Yong-Mei Li, Wen-Min Li, Su-Juan Qin, Qiao-Yan Wen, and Fei Gao. Quantum algorithms for anomaly detection using amplitude estimation. 9 2021. URL <https://arxiv.org/abs/2109.13820v1>.
- [11] Ding Liu and Hui Li. Outlier Detection Using a Novel method: Quantum Clustering. 6 2020. URL <https://arxiv.org/abs/2006.04760v1>.
- [12] Fabio A. González, Alejandro Gallego, Santiago Toledo-Cortés, and Vladimir Vargas-Calderón. Learning with Density Matrices and Random Features. 2 2021. URL <https://arxiv.org/abs/2102.04394v4>.
- [13] Michael A. Nielsen and Isaac L. Chuang. Quantum Computation and Quantum Information: 10th Anniversary Edition. *Quantum Computation and Quantum Information*, 12 2010. doi: 10.1017/CBO9780511976667.
- [14] Marcus Cramer, Martin B. Plenio, Steven T. Flammia, Rolando Somma, David Gross, Stephen D. Bartlett, Olivier Landon-Cardinal, David Poulin, and Yi Kai Liu. Efficient quantum state tomography. *Nature Communications 2010 1:1*, 1(1):1–7, 12 2010. ISSN 2041-1723. doi: 10.1038/ncomms1147. URL <https://www.nature.com/articles/ncomms1147>.
- [15] Daniel F.V. James, Paul G. Kwiat, William J. Munro, and Andrew G. White. On the measurement of qubits. *Asymptotic Theory of Quantum Statistical Inference: Selected Papers*, pages 509–538, 1 2005. ISSN 2469-9942. doi: 10.1142/9789812563071{\\_}0035.
- [16] Alberto Peruzzo, Jarrod McClean, Peter Shadbolt, Man Hong Yung, Xiao Qi Zhou, Peter J. Love, Alán Aspuru-Guzik, and Jeremy L. O’Brien. A variational eigenvalue solver on a photonic quantum processor. *Nature Communications*

- 2014 5:1, 5(1):1–7, 7 2014. ISSN 2041-1723. doi: 10.1038/ncomms5213. URL <https://www.nature.com/articles/ncomms5213>.
- [17] Ali Rahimi and Benjamin Recht. Random features for large-scale kernel machines. In *Advances in Neural Information Processing Systems 20 - Proceedings of the 2007 Conference*, 2009. ISBN 160560352X.
- [18] Fabio A. González, Vladimir Vargas-Calderón, and Herbert Vinck-Posada. Classification with quantum measurements. *Journal of the Physical Society of Japan*, 90(4):044002, 2021. doi: 10.7566/JPSJ.90.044002. URL <https://doi.org/10.7566/JPSJ.90.044002>.
- [19] Yunchao Liu, Srinivasan Arunachalam, and Kristan Temme. A rigorous and robust quantum speed-up in supervised machine learning. *Nature Physics* 2021 17:9, 17(9):1013–1017, 7 2021. ISSN 1745-2481. doi: 10.1038/s41567-021-01287-z. URL <https://www.nature.com/articles/s41567-021-01287-z>.
- [20] Korbinian Kottmann, Friederike Metz, Joana Fraxanet, and Niccolò Baldelli. Variational quantum anomaly detection: Unsupervised mapping of phase diagrams on a physical quantum computer. *Physical Review Research*, 3(4):043184, 12 2021. ISSN 26431564. doi: 10.1103/PHYSREVRSEARCH.3.043184/FIGURES/7/MEDIUM. URL <https://journals.aps.org/prresearch/abstract/10.1103/PhysRevResearch.3.043184>.
- [21] Esma Aïmeur, Gilles Brassard, and Sébastien Gambs. Quantum speed-up for unsupervised learning. *Machine Learning*, 90(2):261–287, 2 2013. ISSN 08856125. doi: 10.1007/S10994-012-5316-5/TABLES/1. URL <https://link.springer.com/article/10.1007/s10994-012-5316-5>.
- [22] Harry Buhrman, Richard Cleve, John Watrous, and Ronald de Wolf. Quantum Fingerprinting. *Physical Review Letters*, 87(16):167902, 9 2001. ISSN 00319007. doi: 10.1103/PhysRevLett.87.167902. URL <https://journals.aps.org/prl/abstract/10.1103/PhysRevLett.87.167902>.
- [23] Hirotada Kobayashi, Keiji Matsumoto, and Tomoyuki Yamakami. Quantum Merlin-Arthur Proof Systems: Are Multiple Merlins More Helpful to Arthur? *Lecture Notes in Computer Science (including subseries Lecture Notes in Artificial Intelligence and Lecture Notes in Bioinformatics)*, 2906:189–198, 2003. ISSN 16113349. doi: 10.1007/978-3-540-24587-2\_{\\_}21. URL [https://link.springer.com/chapter/10.1007/978-3-540-24587-2\\_21](https://link.springer.com/chapter/10.1007/978-3-540-24587-2_21).
- [24] Lukasz Cincio, Yiğit Subaşı, Andrew T. Sornborger, and Patrick J. Coles. Learning the quantum algorithm for state overlap. *New Journal of Physics*, 20(11):113022, 11 2018. ISSN 1367-2630. doi: 10.1088/1367-2630/AAE94A. URL <https://iopscience.iop.org/article/10.1088/1367-2630/aae94ahttps://iopscience.iop.org/article/10.1088/1367-2630/aae94a/meta>.
- [25] Aku Kammonen, Jonas Kiessling, Petr Plecháč, Mattias Sandberg, and Anders Szepeszy. Adaptive random fourier features with metropolis sampling. *Foundations of Data Science*, 2(3):309–332, 2020.

- [26] Yuqi Liu, Yonghui Xu, Jingli Yang, and Shouda Jiang. A Polarized Random Fourier Feature Kernel Least-Mean-Square Algorithm. *IEEE Access*, 7:50833–50838, 2019. ISSN 21693536. doi: 10.1109/ACCESS.2019.2909304.
- [27] Yoram Baram. Learning by kernel polarization. *Neural Computation*, 17(6):1264–1275, 6 2005. ISSN 08997667. doi: 10.1162/0899766053630341.
- [28] Fanghui Liu, Xiaolin Huang, Yudong Chen, Jie Yang, and Johan A.K. Suykens. Random Fourier Features via Fast Surrogate Leverage Weighted Sampling. *Proceedings of the AAAI Conference on Artificial Intelligence*, 34(04):4844–4851, 4 2020. ISSN 2374-3468. doi: 10.1609/AAAI.V34I04.5920. URL <https://ojs.aaai.org/index.php/AAAI/article/view/5920>.
- [29] Raj Agrawal, Trevor Campbell, Jonathan Huggins, and Tamara Broderick. Data-dependent compression of random features for large-scale kernel approximation. *AISTATS 2019 - 22nd International Conference on Artificial Intelligence and Statistics*, 10 2018. doi: 10.48550/arxiv.1810.04249. URL <https://arxiv.org/abs/1810.04249v2>.
- [30] Kun Fang, Xiaolin Huang, Fanghui Liu, and Jie Yang. End-to-end Kernel Learning via Generative Random Fourier Features. 9 2020. doi: 10.48550/arxiv.2009.04614. URL <https://arxiv.org/abs/2009.04614v2>.
- [31] Yang Li, Si Si, Gang Li, Cho-Jui Hsieh, and Samy Bengio. Learnable Fourier Features for Multi-Dimensional Spatial Positional Encoding. 6 2021. doi: 10.48550/arxiv.2106.02795. URL <https://arxiv.org/abs/2106.02795v3>.
- [32] Jiaxuan Xie, Fanghui Liu, Kaijie Wang, and Xiaolin Huang. Deep Kernel Learning via Random Fourier Features. 10 2019. doi: 10.48550/arxiv.1910.02660. URL <https://arxiv.org/abs/1910.02660v1>.
- [33] Xiantong Zhen, Haoliang Sun, Yingjun Du, Jun Xu, Yilong Yin, Ling Shao, and Cees Snoek. Learning to Learn Kernels with Variational Random Features. *37th International Conference on Machine Learning, ICML 2020*, PartF16814:11346–11356, 6 2020. doi: 10.48550/arxiv.2006.06707. URL <https://arxiv.org/abs/2006.06707v2>.
- [34] Eduard Gabriel Băzăvan, Fuxin Li, and Cristian Sminchisescu. Fourier Kernel Learning. *Lecture Notes in Computer Science (including subseries Lecture Notes in Artificial Intelligence and Lecture Notes in Bioinformatics)*, 7573 LNCS(PART 2):459–473, 2012. ISSN 03029743. doi: 10.1007/978-3-642-33709-3\_{\\_}33. URL [https://link.springer.com/chapter/10.1007/978-3-642-33709-3\\_33](https://link.springer.com/chapter/10.1007/978-3-642-33709-3_33).
- [35] Chun Liang Li, Wei Cheng Chang, Youssef Mroueh, Yiming Yang, and Barnabás Póczos. Implicit Kernel Learning. *AISTATS 2019 - 22nd International Conference on Artificial Intelligence and Statistics*, 2 2019. doi: 10.48550/arxiv.1902.10214. URL <https://arxiv.org/abs/1902.10214v1>.
- [36] Brian Bullins, Cyril Zhang, and Yi Zhang. Not-So-Random Features. *6th International Conference on Learning Representations, ICLR 2018 - Conference*

- Track Proceedings*, 10 2017. doi: 10.48550/arxiv.1710.10230. URL <https://arxiv.org/abs/1710.10230v2>.
- [37] Murray Rosenblatt. Remarks on Some Nonparametric Estimates of a Density Function. <https://doi.org/10.1214/aoms/1177728190>, 27(3):832–837, 9 1956. ISSN 0003-4851. doi: 10.1214/AOMS/1177728190.
- [38] Emanuel Parzen. On Estimation of a Probability Density Function and Mode. *The Annals of Mathematical Statistics*, 33(3):1065 – 1076, 1962. doi: 10.1214/aoms/1177704472. URL <https://doi.org/10.1214/aoms/1177704472>.
- [39] Raban Iten, Roger Colbeck, Ivan Kukuljan, Jonathan Home, and Matthias Christandl. Quantum circuits for isometries. *Phys. Rev. A*, 93:032318, Mar 2016. doi: 10.1103/PhysRevA.93.032318. URL <https://link.aps.org/doi/10.1103/PhysRevA.93.032318>.
- [40] Mikko Möttönen, Juha J. Vartiainen, Ville Bergholm, and Martti M. Salomaa. Transformation of quantum states using uniformly controlled rotations. *Quantum Info. Comput.*, 5(6):467–473, sep 2005. ISSN 1533-7146.
- [41] Diego H. Useche, Andres Giraldo-Carvajal, Hernan M. Zuluaga-Bucheli, Jose A. Jaramillo-Villegas, and Fabio A. González. Quantum measurement classification with qudits. *Quantum Information Processing 2021 21:1*, 21(1):1–12, 12 2021. ISSN 1573-1332. doi: 10.1007/S11128-021-03363-Y. URL <https://link.springer.com/article/10.1007/s11128-021-03363-y>.
- [42] Vladimir Vargas-Calderón, Fabio A. González, and Herbert Vinck-Posada. Optimisation-free Classification and Density Estimation with Quantum Circuits. 3 2022. doi: 10.48550/arxiv.2203.14452. URL <https://arxiv.org/abs/2203.14452v2>.
- [43] Charu C. Aggarwal and Saket Sathe. Theoretical Foundations and Algorithms for Outlier Ensembles. *ACM SIGKDD Explorations Newsletter*, 17(1):24–47, 9 2015. ISSN 1931-0145. doi: 10.1145/2830544.2830549. URL <https://dl.acm.org/doi/abs/10.1145/2830544.2830549>.
- [44] John Preskill. Quantum Computing in the NISQ era and beyond. *Quantum*, 2:79, 8 2018. ISSN 2521327X. doi: 10.22331/q-2018-08-06-79. URL <https://quantum-journal.org/papers/q-2018-08-06-79/>.